LABORATORI NAZIONALI DI FRASCATI
SIS – Pubblicazioni

LNF-03/013 (R)
25 Agosto 2003

STUDIES ON A BI-PERIODIC X-BAND STRUCTURE FOR SPARC

D. Alesini [1], A.Bacci[2], M.Migliorati[3], A.Mostacci[3], L.Palumbo[3] and B.Spataro[1]

[1)] INFN-LNF,Via E.Fermi 40, I-00044 Frascati (RM)
[2)] INFN-LASA di Milano – Via Fratelli Cervi 201, I-20090 Segrate (MI)
[3)] INFN-LNF and Università di Roma"La Sapienza", Dip. Energetica-Via A. Scarpa 14, I-00161 Roma

Abstract

The paper presents the design of a compact bi-periodic accelerating section, operating at the frequency of 11.424 GHz, for linearizing the longitudinal phase space in the Frascati Linac Coherent Light Source (SPARC). The structure operates on the $\pi/2$ standing wave mode with axial coupled cavities, and it is designed to obtain a 5 MV accelerating voltage.

The proposed accelerating section represents an alternative design to the standard π-mode cavity, having some advantages as discussed in the paper. Numerical simulations have been carried out with SUPERFISH, OSCARD2D and ABCI codes, in frequency and in time domain. The study includes: field profile optimization, quality factor and shunt impedance calculation, analysis of the generator-cavity coupling and thermal analysis.

1 INTRODUCTION

In order to achieve, in the SPARC project, a linear longitudinal phase space bunch configuration, the use of an additional X-Band microwave accelerating section is needed[1)]. A possible schematic layout to be used for this linearization is reported in Fig 1. In the scheme:

a) the photo-cathode RF gun, which works at a frequency f_{GUN} = 2.856 GHz, delivers bunches with a 5 MeV energy, 1 nC charge and 10 psec bunch length;
b) the X-Band accelerating structure works at a frequency $f_{CAV} = 4*f_{GUN}$;
c) the S-Band travelling wave velocity bunching works at a frequency f_{COMPR} = 2.856 GHz;
d) two $2\pi/3$ travelling wave constant gradient structures operate at a frequency f = 2.856 GHz.

The use of an X-Band structure is required to compensate the non-linear distortions due to the RF curvature during acceleration and RF compression. Numerical analysis of the beam transport with the combined action of the X-Band microwave structure and of the bunch compressor are still under study.

The beam dynamics of the system is not affected by the long-range wake-fields because the scheme operates with single bunches. As a consequence no dedicated dampers of the parasitic higher order modes of the X-Band section have been adopted.

The advantages in the use of X-Band structures are well known: reduced sizes, higher shunt impedances, higher breakdown threshold levels and short fill times. Moreover, the technologies in the X-Band accelerating structures, high power sources and modulators have been already developed at KEK[2), 3)], SLAC[4), 5), 6)] and Varian[7), 8)] for future linear collider projects.

A basic consideration in the choice of the operating mode is the sensitivity of the cavity field distribution and frequency with respect to the machining errors. In fact field flatness is needed for beam dynamic requirements and for obtaining maximum net accelerating voltage with a tolerable peak surface field. This subject has been already treated applying the perturbation theory to the equivalent circuit of a multi-cell structure[9)] or considering the multiple reflection of a wave traveling on a finite chain of coupled resonators[10)] including also the presence of the beam loading[11)].

The required mechanical tolerances increase the complexity of the machining and alignment tolerances and such important aspects have to be taken into account in the design activity. From this point of view the $\pi/2$ mode gives less sensitivities with respect to the global machining errors if compared with a π mode operating cavity. It also reduces the parasitic effects given from the beam cumulative break-up instabilities. On the contrary, it gives lower shunt impedance per unit length and major fabricating costs because of the presence of the coupling cells.

In the following we discuss the detailed design procedure of the X-Band structure consisting in: field profile optimization, form factor (R_{sh}/Q) and quality factor (Q)

calculations, power losses evaluation, dispersion curve analysis, cooling system estimations, electric field breakdown calculation.

2 CHOICE OF THE ACCELERATING STRUCTURE TYPE

As already mentioned in [12] the design of new generation accelerating sections is defined in a broader perspective by resulting from a compromise of among several factors: beam dynamics requirements, RF power sources, fabrication constraints, sensitivity to machining errors and so on. The global RF requests in the accelerating SW structures design are summarized in the following[8]:

1) high accelerating field gradient to reduce the accelerator length;
2) high shunt impedance to reduce the requirement of RF power;
3) low ratios E_p/E_0 and B_p/E_0 (where E_p and B_p represent the surface peak electric and magnetic fields respectively and E_0 is the average accelerating field) to reduce dark currents, break down conditions and thermal effects;
4) high group velocity in order to be less sensitive to the mechanical fabrications errors;
5) low content of longitudinal and transverse higher order modes that can affect the beam dynamics;
6) appropriate shape profile to avoid multipactoring phenomena that could limit the accelerating section performances.

Our main concern is to design an accelerating structure with the requirements reported below :

1) accelerating voltage V = 5 MV ;
2) length L = 12 cm ;
3) beam aperture hole ϕ = 8 mm;
4) operating frequency f_{CAV} = 11.424 GHz;

with the following beam parameters:

1) pulse charge, Q = 1 nC;
2) full pulse length, τ = 10 psec;
3) single pulse operation;
4) pulse repetition rate frequency, f_{REP} = 50 Hz.

A general bi-periodic structure can be designed with side-coupling cells or axial coupling cells[13]. Since the side-coupled cavities increase the number matching and assembly steps[14], the present design is addressed to use a bi-periodic with axial coupled cells.

Standing wave bi-periodic sections operating in the $\pi/2$ mode have been studied by many authors and used for electron linear accelerators in the S-band frequency range.

The main advantage of such structures is the reduced sensitivity of the field flatness and the resonant frequency with respect to the mechanical errors, cell-to-cell temperature variations and assembly errors. On the other hand, as we will illustrate later, they have shunt impedance per unit length slightly reduced with respect to the π mode structure. Moreover the process of tuning is more difficult because it is necessary to close the so-called stop-band.

In our case from the beam loading and beam dynamics point of view, no specific effects have to be expected because of the operation with a small average current and single bunch.

Concerning the dissipated power, the fourth harmonic frequency implies small physical dimensions and, therefore, the dissipated density power constitutes one of the main constraints. A reasonable upper limit on the average power dissipation has been estimated to be around at 4 kW/m. By assuming a 3 MW input peak power with a duty cycle of 10^{-4}, the shunt impedance of 8 MΩ gives the designed average accelerating voltage (5 MV) with 2.5 kW/m dissipated power. The shunt impedance value of 8 MΩ represents, therefore, the minimum value that we have to achieve in the design procedure.

Operation with quality factor Q sufficiently high is also required to prevent the excitation of near unwanted modes.

To simplify the construction procedure a simple geometry has been decided. The structure consists of a chain of cylindrical standard profile accelerating and coupling cavities. These last ones have a reduced length with respect to the accelerating ones because they are necessary for coupling only. In fact, coupling cavities, in the π/2 mode, are not excited to the first order and do not contribute, practically, to beam acceleration. The accelerating cavities periodicity is $p = l = \beta\lambda/2 = 1.312$ cm and the irises thickness (t) is 2 mm. The detailed RF properties and the thermal analysis of the π/2 mode are described in the following.

3 ACCELERATING STRUCTURE RF PROPERTIES

The longitudinal available space, the minimum beam aperture and the operating frequency give the dimensions of the structure reported in Fig. 2(C).

The frequency analysis of the bi-periodic sections constituted by a chain of N accelerating cells and N-1 coupling cells shows several interesting features.

The calculations in frequency domain have been performed using the SUPERFISH[15] and OSCAR2D[16] computation codes.

In order to reduce the computation effort and, contemporary, to increase the precision of the results, preliminary simulations have been carried out on a half period of the cells with symmetry planes as indicated in Fig. 3. The simulation has been performed with the mesh sizes between 0.01 cm and 0.005 cm, of the same order of magnitude of the achievable minimum mechanical tolerances.

The double periodicity of the structure operating on π/2 mode introduces a stop band in the dispersion curve with two π/2 mode configurations, characterized by different fields distribution and frequencies, as reported in Fig. 4. In other words there are two resonant modes with the same cell-to-cell phase shift $\Phi = \pi/2$: one of them excites the long accelerating cavities, the other one excites the short coupling cavities[13].

The calculation of the stop band frequencies of the structure has been done simulating a half cell and imposing boundary conditions as illustrated in Fig. 3. Quantitative checks performed by using the well-known analytical lumped parameter model confirmed the numerical results relative to the two $\pi/2$ modes resonance [17].

To close the stop band, the short cavity radius has been increased up to make equal the resonant frequencies of the two modes. The corresponding field distributions of the accelerating and coupling cells, obtained with Dirichelet/Neumann conditions on the symmetry planes, are reported in Fig. 3.

A careful look at the picture shows that the field of the "nominal" accelerating mode (long cavity) is zero inside the coupling cavity (short cavity), while the field of the non-accelerating mode (short cavity) is zero inside the accelerating cavity (long cavity). It is relevant to remark that this condition is obtained when the stop-band is closed, on the other hand, as it is shown in the same picture, it is possible to note that when the stop-band is opened some field lines enter more in the unexcited cell.

With the dimensions of the bi-periodic structure indicated in Fig. 2(C), we have obtained the form factor per unit length R/(Q*L) and the quality factor Q reported in Tab. 1. Both parameters fulfil the design requirements.

Additional simulations have been carried out to estimate the shunt impedance and the stop band change as function of the coupling-cell length by keeping closed the stop band and unchanged the periodicity of the structure. We have obtained $\Delta r/\Delta L_C = 8$ (MΩ/m)/mm and $\Delta f/\Delta L_C = 900$ (MHz/mm) respectively. The calculation results are shown in Fig. 5.

The sensitivity of the resonant frequency with respect to the external cavity radius has been estimated to be around $\Delta f/\Delta b = 1.2$ MHz/μm while the sensitivity of the resonant frequency as function of the iris radius has been carefully investigated because it affects the stop-band width. It has been calculated a sensitivity of 0.35 MHz/μm for the $\pi/2$ accelerating mode (long cavities) and a different sensitivity of 0.85 MHz/μm for the $\pi/2$ non-accelerating mode (short cavities).

3.1 Accelerating structure dispersion curve calculations

The final structure is constituted by 9 accelerating cells and 8 coupling cells. In Fig. 2(A) and 2(B) we have reported the structure sections, with the symmetry planes (magnetic and electric mirror) that have been simulated to calculate the dispersion curve. The number of cells has been chosen in order to sample the dispersion curve itself in a reasonable number of points. In particular the point corresponding to the $\pi/2$ mode allows to investigate the stop band width as a function of the cell sizes. In Fig. 6 it is shown the dispersion curve obtained from an ideal structure (Fig. 2(B)), compared with the dispersion curve of a structure with beam pipe tubes (Fig. 2(C)). As predictable the beam tubes change slightly the resonant frequency of the individual mode even if the $\pi/2$ mode frequency remain, substantially, unchanged[18].

The separation of the lower and upper cut-off frequencies allows us to determine the bandwidth of the structure.

The calculated coupling coefficient given by [19]:

$$K = \frac{\omega_\pi - \omega_0}{\omega_{\pi/2}} \qquad (1)$$

has been estimated to be about 3.63 %.

For a multi-cell structure, how it is well known, modes that are close in frequency to the operating one can perturb, in a real structure, the field of the operating mode. The increase of the mode separation can give, from this point of view, beneficial effects. A very attractive feature of the π/2 mode is the great closest-mode separation with respect to the other possible operating modes. It has been evaluated to be equal to 125 MHz. This mode separation is more than a factor 10 bigger than those of the π mode[12]. We expect, therefore, reduced perturbation of the accelerating field with respect to the machining errors of the cells or with respect to different temperature working conditions of the cells themselves.

For completeness we have also studied the generator coupling coefficient and the beam-loading of the structure even if, in SPARC project, we work in single bunch operating conditions and we will not be involved on beam-loading effects.

Following the analytic treatment based on the equivalent LRC circuit for a RF source connected to the accelerating structure[20], is it possible to obtain the equation that relates the power dissipated in the cells, the power given by the RF generator, the generator coupling coefficient (β) and the beam-loading parameter (k) in the following way:

$$\sqrt{P_g}\left[\frac{2\sqrt{\beta}}{1+\beta}\left(1-\frac{k}{\sqrt{\beta}}\right)\right] = \sqrt{P_c} \qquad \text{with} \qquad k = \frac{I_0}{2}\sqrt{\frac{R_{sh}}{P_g}} \qquad (2)$$

Where R_{sh} is the shunt-impedance of the structure, P_c is the power dissipated in the cavity, β the coupling coefficient, P_g input generator power and I_0 is the average beam current. The analysis has been done assuming short bunches ($\omega_{RF}\sigma_z << 1$). In Fig. 8 it is plotted the behavior of P_g as a function of the coupling factor β for different beam current values.

3.2 Working mode characteristics

In Fig. 7(A) it is shown the field profile distribution of the accelerating mode of the final multi-cell structure with beam tubes obtained by keeping the end-cells radius identical to the other cells. The field flatness is clearly not achieved, even if the difference between the peak E-field in the end-cells and the peak in the central-cell is quite small (a factor 1.2 grater than the end cells). The reduction of the electric field in the terminal cells is lower than in a π mode case[12] where the ratio between the two peak E field was 3.5. This is because, as we have remarked before, the π/2 mode is less sensitive with respect to cell tuning perturbations.

In order to compensate this longitudinal E-field reduction, it has been followed the procedure adopted by other authors[19]: the end-cells have to be machined with a lower different radius (of the order of 18 μm) as shown in Fig. 7(B).

The obtained shunt impedance per unit length is equal to R_{sh} = 68 MΩ/m. The average dissipated power is ~300 W assuming a peak input power of 3 MW and a 10^{-4} duty cycle.

The peak electric field surface is a factor 6 below that measured at SLAC[7]. The energy spread due to beam loading has been calculated with the analytical expression[21), 22)]:

$$\varepsilon = \frac{bNe\omega_{RF}}{E_{acc}} \frac{R_{sh}}{Q} \tag{3}$$

where bN is the number of particles per beam pulse (consisting of b closely spaced bunches), e is the elementary charge, $\omega_{RF} / 2\pi$ is the RF frequency, E_{acc} is the average accelerating gradient and R_{sh}/Q is the form factor per unit length.

Taking R_{sh}/Q = 9693 Ω/m, bN = 6.24 10^9, E_{acc} = 42 MV/m and f_{RF} = 11.424 GHz, the energy spread is evaluated to be about 0.825%.

We believe that the presence of non-resonant electron loading or dark current gives no specific trouble since the estimation of the average accelerating electric field is 30% lower than the minimum threshold field limit[23].

4 ABCI E MULTI-BUNCH RESULTS

For the multi-bunch operation, a wider analysis in frequency, including higher order modes has to be performed.

In order to get some insight into the electromagnetic interaction between the beam and the structure and, therefore, to obtain the coupling impedance of the structure, we calculated the wake potential of a Gaussian bunch (r.m.s. = 1 mm) over a distance of 3 m behind the bunch by using the well known ABCI code[24), 25)]. The Fourier transform of the wake potential yields the real and imaginary part of the impedance for the bi-periodic structure. Comparing these results with the π mode operation keeping unchanged the periodicity of the structure and the iris thickness, one observes an increased frequency shift of the longitudinal higher modes depending on the axial cell length. In this case, if a line of the beam spectrum would coincide with the frequency of the parasitic resonances, the detuning effects on the beams stability and the power deposition of the beam into the section should be significantly reduced against the possible dangerous effects of the section operating on π mode.

5 THERMAL ANALYSIS

To maintain the structure dimensions unchanged during operation, a close temperature control during the operation is needed. The main factors that affect the section temperature are the RF power losses, the characteristics of the heat transfer mechanism from the structure to the cooling tubes and the variation in the cooling water temperature.

Estimation has been carried out by using a closed cooling water system in order to keep the operating temperature at 40 °C. A preliminary thermal analysis of the structure has been determined by means of the ANSYS[26] software. Fig. 9 depicts the thermal flux on the boundary structure and the distribution in temperature assuming to use copper.

The frequency shift behavior versus the heating of the structure has been studied by the integration between ANSYS and SUPER-FISH. A temperature variation $\Delta T = 1$ °C causes a 191 kHz frequency shift by assuming an isotropic expansion and a 80 kHz frequency shift if one considers the real power distribution shown in the Fig. 9. The maximum dissipated power on the surface is 3.5 W/cm^2.

These results show that temperature stabilization within 0.1 °C has to be applied at the maximum duty cycle to keep the structure frequency within 1/100 of the frequency bandwidth. Additional checks on this topics are still in progress, and more detailed studies will be examined and described in a forthcoming paper.

6 CONCLUSION

In this paper the design of a bi-periodic SW structure operating on the $\pi/2$ mode at 11.424 GHz has been presented.

To simplify the mechanical construction the structure has been designed with axial coupled cells and simple geometry. The external radius of the coupling cells has been tuned to close the stop-band between the two possible $\pi/2$ accelerating modes. The sensitivities of the stop-band width and the $\pi/2$ mode frequency with respect to the structure dimensions have been calculated.

Compared with the π mode structure this accelerating section shows a bigger mode separation (a factor 10 in frequency) with respect to the closest modes. This gives less sensitivity of the field profile with respect to the machining errors and to different operation condition of the cells. On the contrary the presence of the coupling cells complicates the machining and assembling of the structure itself.

The study of the peak electric field shows that we are below the multipacting or dark current threshold.

For completeness, multi-bunch operation condition and the beam loading effects have also been discussed.

A preliminary thermal analysis has been, finally, done showing that a 0.1 °C thermal stabilization in temperature has to be required to keep the structure in resonance.

7 ACKNOWLEDGEMENTS

Useful discussions with R. Parodi are gratefully acknowledged.

REFERENCES

(1) M. Ferrario, private communications.
(2) S. Takeda et al., Particle Accelerator, 30 (1990), 1101.
(3) K. Takata, Proc. First Workshop on Japan Linear Collider (JLC), KEK, Oct. 24-25, 1989, 2.
(4) J. W. Wang and G. A. Loew, "Measurements of ultimate Accelerating Gradients in the SLAC Disk-loaded Structure", 1985 PAC, Vancouver, May 1985, SLAC-PUB-3597, March 1985.
(5) J. W. Wang, V. Nguyen-Tuong and G. A. Loew, " RF Breakdown Studies in a SLAC Disk-loaded Structure", Proceedings of the 1986 Linear Accelerator Conference, Stanford, Ca, June 1986, SLAC-PUB-3940, April 1986.
(6) J. W. Wang and G. A. Loew, "Progress Report on New RF Breakdown Studies in an S-band Structure at SLAC", presented at the 1987 PAC, Washington D.C., March 1987, SLAC-PUB-4247, February 1987.
(7) E. Tanabe, J. W. Wang and G. A. Loew, "Voltage Breakdown at X-band and C-band Frequencies", Proceedings of the 1986 Linear Accelerator Conference, Stanford, Ca, June 1986; E. Tanabe, "Breakdown in High-Gradient Accelerators Cavities", Proceedings of the 1984 Linear Accelerator Conference, Seeheim/Darmstadt, West Germany, p.403, May 1984.
(8) J. W. Wang, "RF Properties of Periodic Accelerating structures for Linear Colliders", SLAC-Report-339, July 1989.
(9) J. R. Rees, "A Perturbation Approaach to Calculating the behavior of Multi-cell Radiofrequency Accelerating Structures", PEP-255, Stanford Linear Accelerator Centre (1976).
(10) P. B. Wilson, IEEE Trans. Nucl. Sci. NS-16, No. 3, 1092 (1969).
(11) T. Nishikava, IEEE Trans. On Nuc. Sci., NS-12 n. 3, 630 (1965).
(12) A. Bacci et al., "An X-band structure for a longitudinal emittance correction at SPARC", SIS PUB LNF 03/008 (R), LNF, 2003.
(13) P. Fernandes, R. Parodi, B. Spataro, F. Tazzioli and D. Tronc," Field Computation and Measurements on a Biperiodic Buncher Structure", 1986 Linear Accelerator Conference, SLAC, Stanford University, Stanford, California-June 2-6, 1986
(14) E. Tanabe, M. Bayer, and M. Trail, IEEE Trans. Nucl. Sci., NS-32, 2975 (1985).
(15) Poisson Superfish, James H. Billen and Lloyd M. Young, software produced under U.S. Government by Los Alamos National Laboratory, Particle Accelerators 7 (4), 213-222 (1976).
(16) P. Fernandes and R. Parodi, "LALAGE – A Computer Program to Calculate the TM Modes of Cylindrically Symmetrical Multicell Resonant Structures", PAC 1982, Vol. 12, pp. 131-137.
(17) D. E. Nagle, E. A. Knapp and B. C. Knapp, Rev. Sci. Instr. **38**, 1583 (1967); E. A. Knapp, B. C. Knapp and J. M. Potter, Rev. Sci. Instr. **39**, 979 (1968)
(18) H. Padamsee, J. Knobloch, T. Hays, "RF Superconductivity for Accelerators", John Wiley & Sons, (pages 131-133).
(19) P. Fernandes and R. Parodi,"On Compensation of Field Unflatness of Axial Electric Field in Multi-cell Resonant Structures", Particle Accelerators **14**,(1984).
(20) P. B. Wilson "High Energy Electron Linacs: Applications to Storage Ring RF Systems and Linear Colliders", SLAC-PUB-2884 (rev.) 1991.
(21) W. Schell,"Dissipation Versus Peak Power in a Classical Linac", LEP-RF/WS/ps, CLIC note 4, 22nd October 1985.

(22) P. Brunet, ”Section Accelerateur Fort Courant en Ondes Stationnaires”, LAL/PI/80-20, Orsay May 1980.
(23) G. Bienvenu, P. Fernandes and R. Parodi,”An Investigation on the Field Emitted Electrons in Traveling Wave Accelerating Structure”, NIM A320 (1992) 1-8.
(24) Y. H. Chin, CERN LEP-TH/88-3,1988.
(25) Y.H. Chin,”Advances and Applications of ABCI”, 1993 PAC Washington D.C., May 17-20, 1993.
(26) ANSYS is a simulation software used to determine real-world structural, thermalelectromagnetic and fluid-flow behavior of 3-D product designs. www.ansys.com

Tab. 1: RF parameter list of the standing wave bi-periodic structure working on the π/2 mode as obtained by SUPERFISH and OSCAR 2D codes

-Frequency, f (MHz)	11431.57*
-Length for calculation, L (cm)	11.509
-Beam tube length, 1 (cm)	3
-Cavities number, n_b	9**
-Ratio of phase to light velocity, v_ϕ/c	1
-Structure periodicity, L_p (cm)	1.3121
-Beam hole radius, r (cm)	0.4
-Iris Thickness, t(cm)	0.2
-Transit time factor, T	0.765
-Factor of merit, Q	7101
-Form factor, R_{sh}/Q (Ω/m)	9693
-Shunt impedance per unit length, R_{sh} (M Ω/m)	68.83
-Coupling coefficient K	3.63%
-Peak power, P (MW)	2.949
-Energy stored in cavity of length L, W (joules)	0.292
-Peak power per meter, P/m (MW/m)	25.62
-Energy stored in cavity per meter, W/m (joules/m)	2.537
-Duty cycle, D.C.	10^{-4}
-Repetition frequency, f (Hz)	50
-Power dissipation, P_d (Watt)	294.9
-Average accelerating field, E_{acc}(MV/m)	42
-Peak axial electric field, E_{max} (MV/m)	54.91
-Kilpatrick factor	1.16
-Peak surface electric field, E_{sur} (MV/m)	102.097
-Ratio of peak to average fields E_{max}/E_{acc}	1.31
-Ratio of peak to average fields E_{sur}/E_{acc}	2.431
-Ratio of peak fields B_{max}/E_{sur}(mT/MV/m)	1.9
-Pulse charge, C (nC)	1
-Pulse length, τ (psec)	10
-Bunches number, n	1
-Average beam power, P_{baver} (W)	0.242
-Energy spread due to the beam loading, %	±0.828
-Loss parameters due to the HOM's K_p (V/pC)	16.44
-Loss parameter of the operating mode, K_0 (V/pC)	20.03

*Mesh 0.03 cm. With a mesh of 0.01 cm, we have too long calculation time, but we have seen that the frequency value converge to 11424 MHz

**Number of accelerating cells

Figures caption

Fig. 1 Layout of the first part of the X-FEL SPARC project. The X-band structure allows to correct, locally, the RF curvature and allows to avoid the increase of the longitudinal emittance that can limit the current growing.

Figs. 2 Shape and dimensions of the simulated structures.

Fig. 3 Half-cell simulated structure with the different configuration of the accelerating and no-accelerating electric field lines when the stop band is opened or closed.

Fig. 4 Dispersion curve in case of opened stop-band.

Fig. 5 Shunt impedance and stop-band sensitivity as function of the coupling-cell length by keeping closed the stop-band and unchanged the periodicity of the structure.

Fig. 6 Dispersion curve obtained from the ideal structure, compared with the dispersion curve of the structure with beam pipe tubes.

Fig. 7 Electric field profile of the accelerating mode: (A) structure with beam pipe tubes and with a constant cavity radius; (B) structure with beam pipe tube and with the end-cells engineered with a different radius in order to increase the field flatness.

Fig. 8 Power supplied by the generator (P_g) versus different currents values. It is relevant to note that, in the SPARC case, the beam-loading effects are negligible and one obtains the minimum of the supply power whit a coupling coefficient equal to one.

Fig. 9 Thermal flux on the boundary structure and temperature distribution inside the copper cavity (Studied performed by ANSYS).

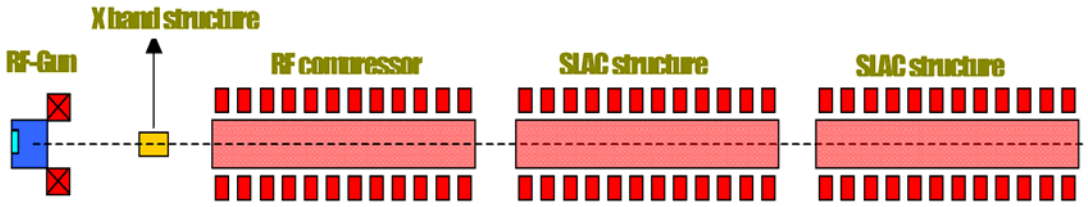
X band structure
RF-Gun
RF compressor
SLAC structure
SLAC structure

Fig 1

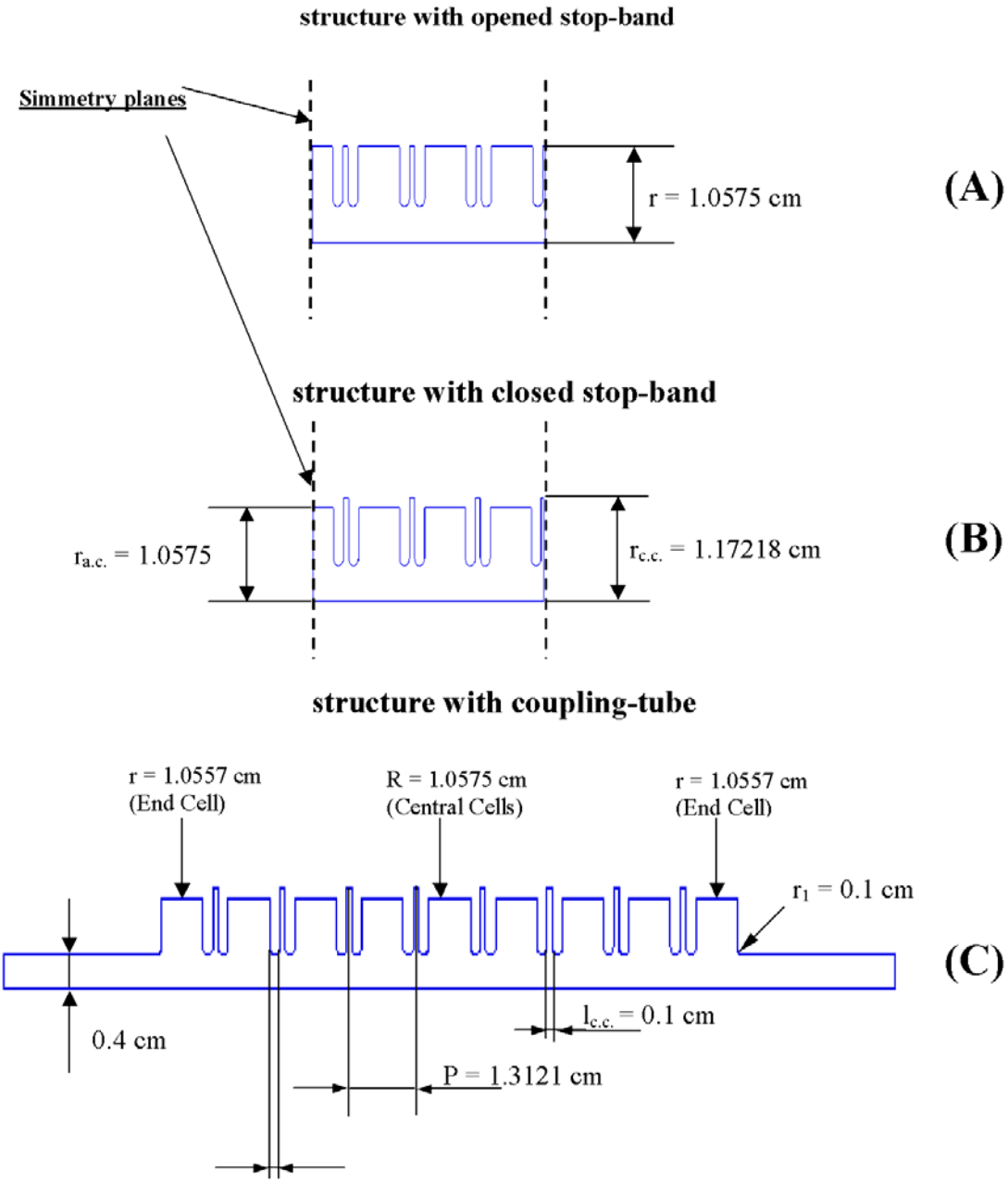
structure with opened stop-band
Simmetry planes
r = 1.0575 cm
(A)
structure with closed stop-band
$r_{a.c.}$ = 1.0575
$r_{c.c.}$ = 1.17218 cm
(B)
structure with coupling-tube
r = 1.0557 cm
(End Cell)
R = 1.0575 cm
(Central Cells)
r = 1.0557 cm
(End Cell)
r_1 = 0.1 cm
0.4 cm
$l_{c.c.}$ = 0.1 cm
P = 1.3121 cm
(C)

Fig. 2

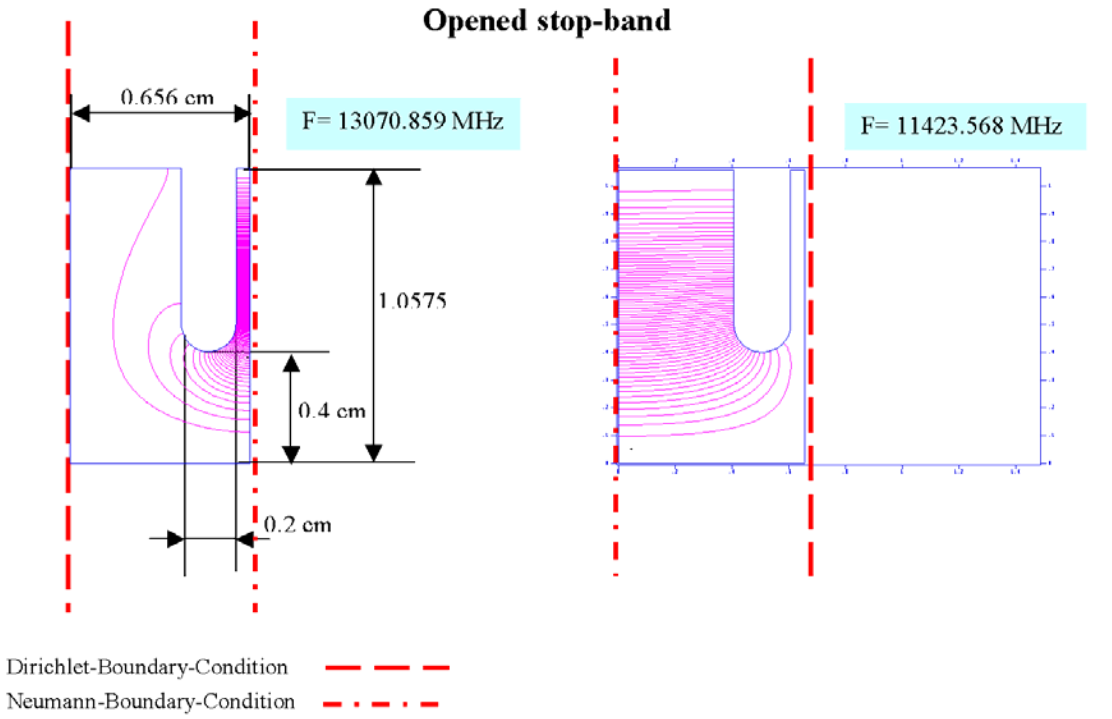
Opened stop-band
0.656 cm
F= 13070.859 MHz
1.0575
0.4 cm
0.2 cm
F= 11423.568 MHz
Dirichlet-Boundary-Condition
Neumann-Boundary-Condition

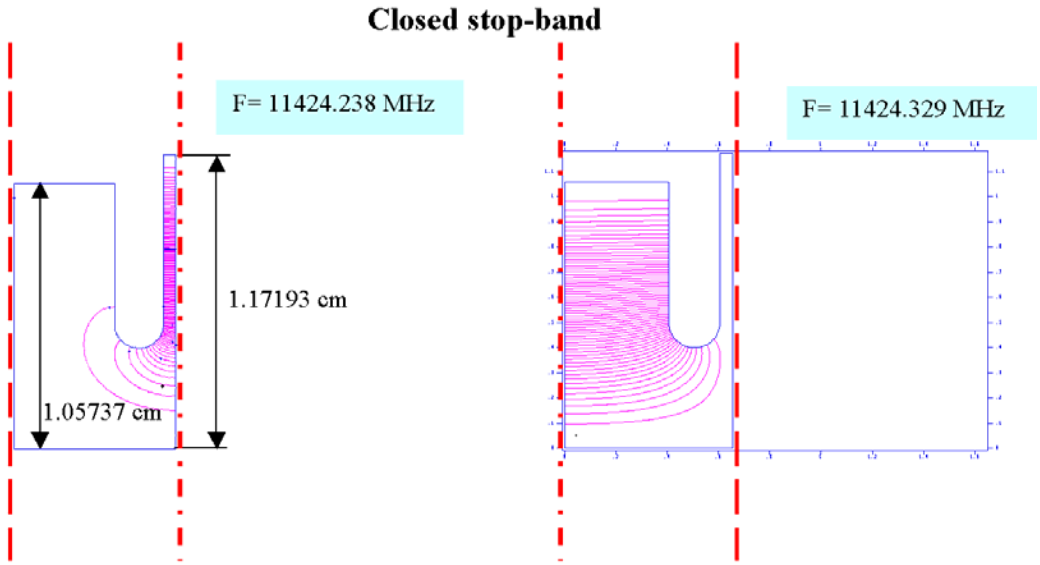
Closed stop-band
F= 11424.238 MHz
1.17193 cm
1.05737 cm
F= 11424.329 MHz

Fig. 3

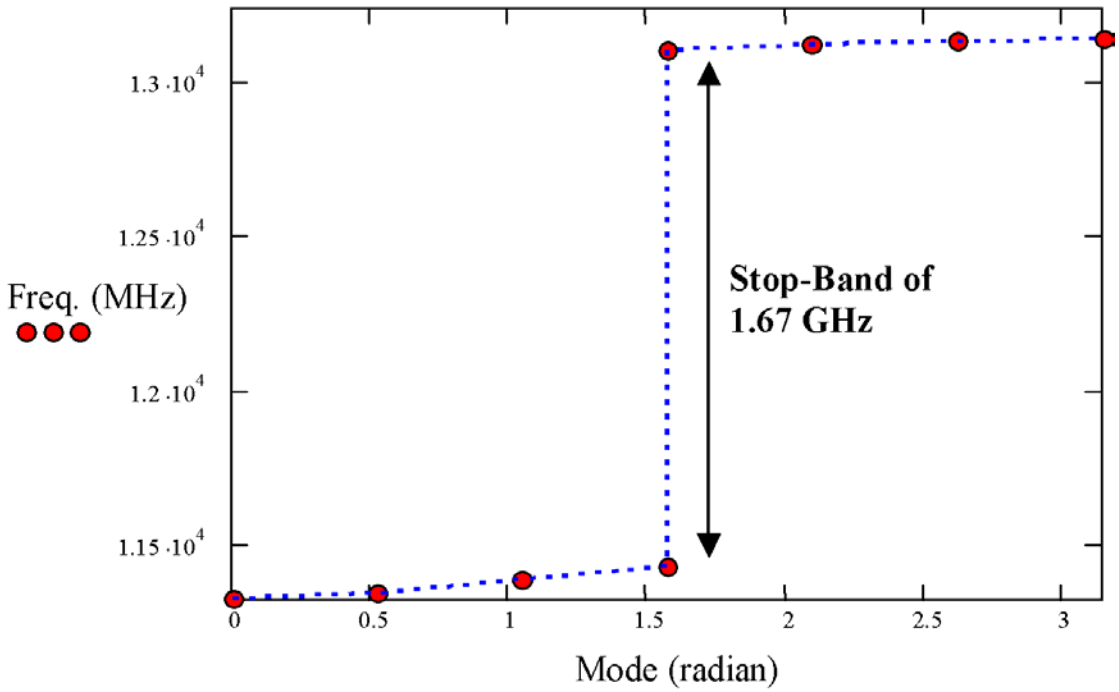

Fig. 4

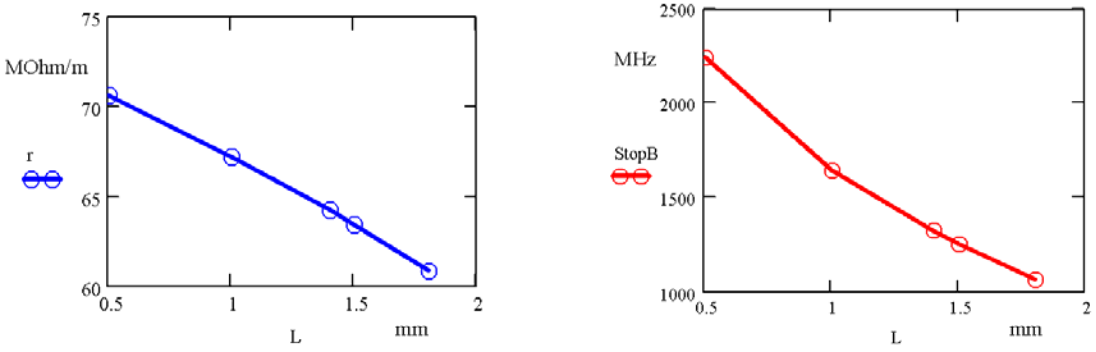

Fig.5

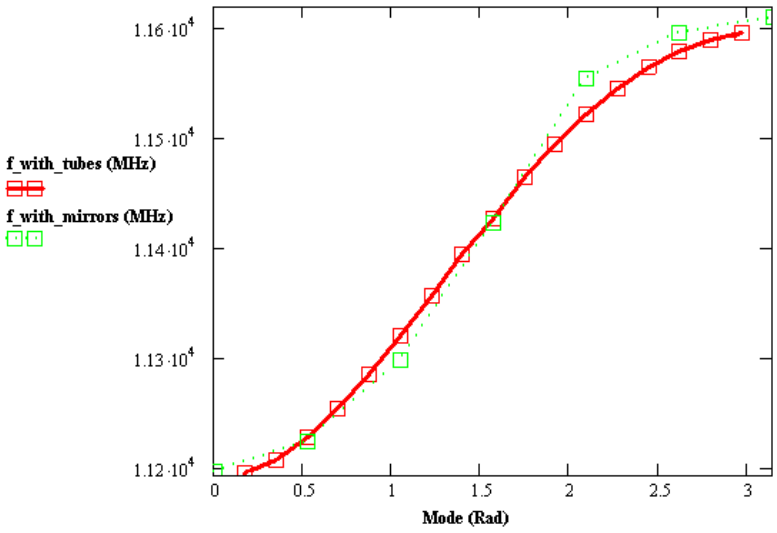

Fig. 6

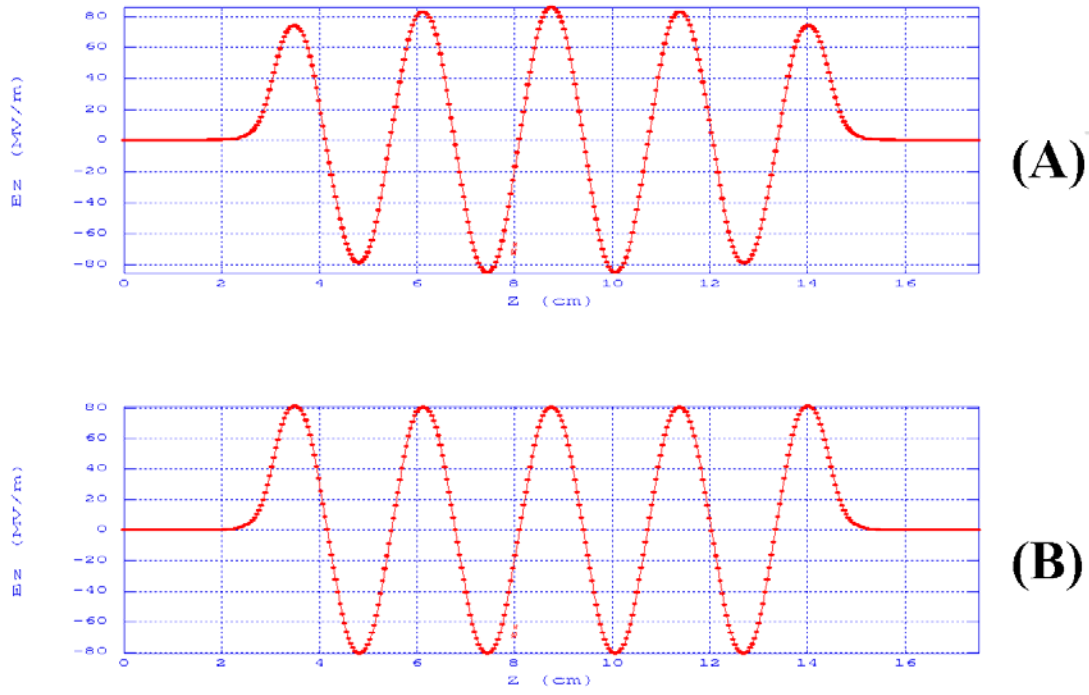

Fig. 7

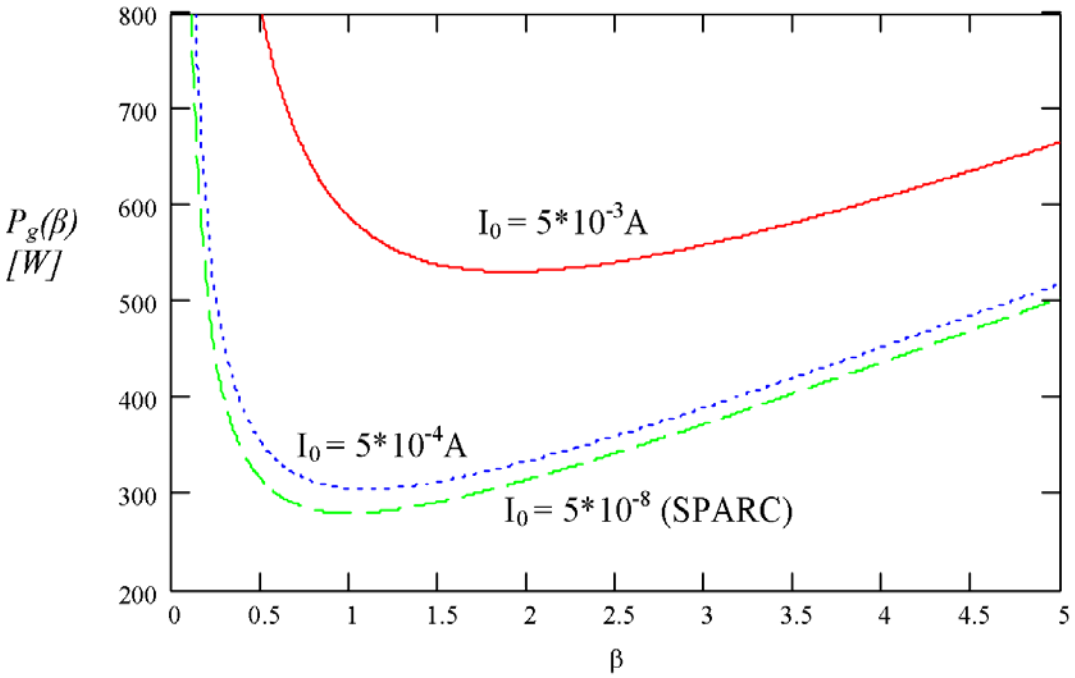

Fig. 8

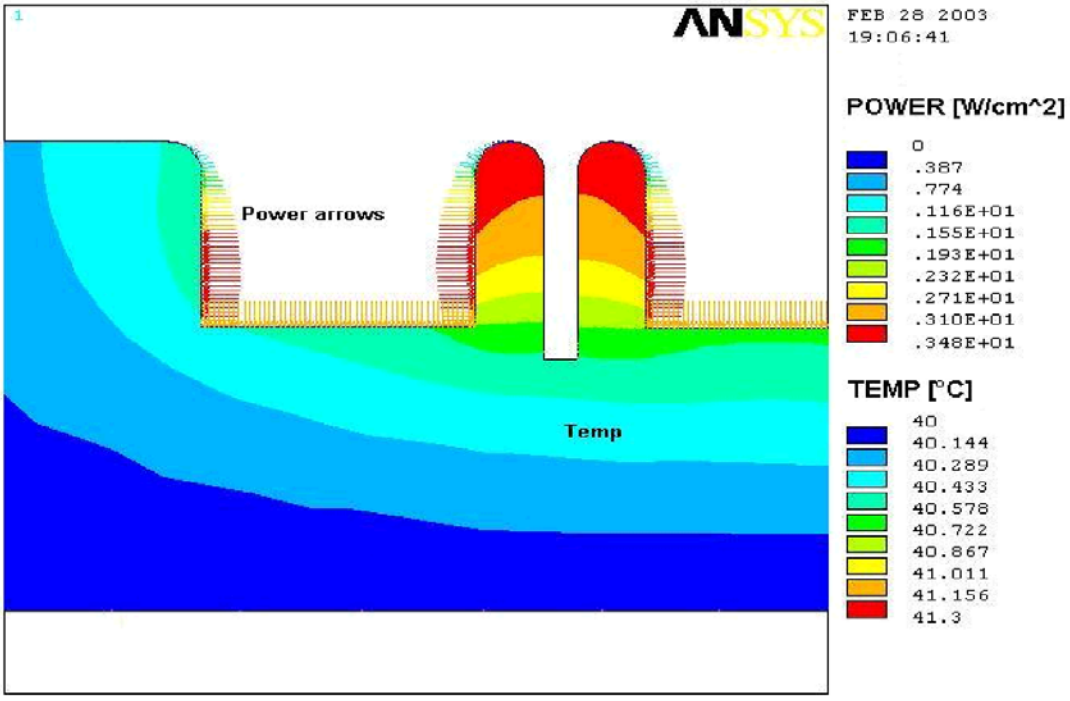
1
ANSYS
FEB 28 2003
19:06:41
POWER [W/cm^2]
0
.387
.774
.116E+01
.155E+01
.193E+01
.232E+01
.271E+01
.310E+01
.348E+01
TEMP [°C]
40
40.144
40.289
40.433
40.578
40.722
40.867
41.011
41.156
41.3
Power arrows
Temp

Fig. 9